The Breast 49 (2020) 174–182

Contents lists available at ScienceDirect

The Breast

journal homepage: www.elsevier.com/brst

Original article

Preoperative assessment of breast cancer: Multireader comparison of contrast-enhanced MRI versus the combination of unenhanced MRI and digital breast tomosynthesis

Rossano Girometti [a, *], Valentina Marconi [a], Anna Linda [a], Luisa Di Mico [a], Federica Bondini [a], Chiara Zuiani [a], Francesco Sardanelli [b, c]

[a] Institute of Radiology, Department of Medicine, University of Udine, University Hospital "S. Maria Della Misericordia", P.le S. Maria Della Misercordia N, 15, 33100, Udine, Italy
[b] Radiology Unit, IRCCS Policlinico San Donato, Milan, Italy
[c] Department of Biomedical Sciences for Health, Università Degli Studi di Milano, Milan, Italy

ARTICLE INFO

Article history:
Received 7 September 2019
Received in revised form
22 November 2019
Accepted 26 November 2019
Available online 4 December 2019

Keywords:
Breast neoplasms
Neoplasm staging
Sensitivity
Digital breast tomosynthesis
Magnetic resonance imaging

ABSTRACT

Purpose: To compare the sensitivity for breast cancer (BC) and BC size estimation of preoperative contrast-enhanced magnetic resonance imaging (CEMRI) versus combined unenhanced magnetic resonance imaging (UMRI) and digital breast tomosynthesis (DBT).
Patients and methods: We retrospectively included 56 women who underwent DBT and preoperative 1.5 T CEMRI between January 2016–February 2017. Three readers with 2–10 years of experience in CEMRI and DBT, blinded to pathology, independently reviewed CEMRI (diffusion-weighted imaging [DWI], T2-weighted imaging, pre- and post-contrast T1-weighted imaging) and a combination of UMRI (DWI and pre-contrast T1-weighted imaging) and DBT. We calculated per-lesion sensitivity of CEMRI and UMRI + DBT, and the agreement between CEMRI, UMRI and DBT versus pathology in assessing cancer size (Bland-Altman analysis). Logistic regression was performed to assess features predictive of cancer missing.
Results: We included 70 lesions (64% invasive BC, 36% ductal carcinoma in situ or invasive BC with in situ component). UMRI + DBT showed lower sensitivity (86–89%) than CEMRI (94–100%), with a significant difference for the most experienced reader only ($p = 0.008$). False-positives were fewer with UMRI + DBT (4–5) than with CEMRI (18–25), regardless of the reader ($p = 0.001$–0.005). For lesion size, UMRI showed closer limits of agreement with pathology than CEMRI or DBT. Cancer size $\leq$1 cm was the only independent predictor for cancer missing for both imaging strategies (Odds ratio 8.62 for CEMRI and 19.16 for UMRI + DBT).
Conclusions: UMRI + DBT showed comparable sensitivity and less false-positives than CEMRI in the preoperative assessment of BC. UMRI was the most accurate tool to assess cancer size.

1. Introduction

Contrast-enhanced magnetic resonance imaging (CEMRI) has emerged as the most reliable tool for assessing loco-regional extent of breast cancer (BC). Based on superior contrast resolution and the capability of exploiting tumoral neoangiogenesis [1], CEMRI is highly sensitive in detecting multicentric, multifocal and bilateral cancer foci [2,3], as well as in predicting BC size at pathology [4–6]. Despite this, the impact on surgical outcomes of preoperative CEMRI is disputed [7,8]. On the other hand, this technique is increasingly used for tailoring the surgical approach [9].

There are several disadvantages limiting the widespread adoption of CEMRI. First, examination specificity is generally regarded as suboptimal for the purpose of minimizing overdiagnosis and overtreatment of false-positive (FP) findings, even though second-

* Corresponding author.
E-mail addresses: rgirometti@sirm.org, rossano.girometti@uniud.it (R. Girometti), vale.marconi27@gmail.com (V. Marconi), anna.linda@asuiud.sanita.fvg.it (A. Linda), luisa.dimico@gmail.com (L. Di Mico), federica.bondini@gmail.com (F. Bondini), chiara.zuiani@uniud.it (C. Zuiani), francesco.sardanelli@unimit.it (F. Sardanelli).

https://doi.org/10.1016/j.breast.2019.11.013

Abbreviations

BC	breast cancer
CEMRI	contrast enhanced Magnetic resonance imaging
DBT	Digital breast tomosynthesis
UMRI	unenhanced Magnetic resonance imaging
R1-R3	readers 1 to 3
IQR	(interquartile range)
ICC	Intraclass correlation coefficient

look ultrasound [10–12] and MRI-guided biopsy [13] enable to solve these limitations. Second, concerns exist in terms of accessibility and availability, costs, and need for expertise, thus limiting the use of preoperative CEMRI to selected centres [9]. Finally, contrast administration is associated with the risk of hypersensitivity reactions, systemic nephrogenic fibrosis, and accumulation/retention in the central nervous system and other body areas [14,15].

There is an ever-increasing interest in technical variants of the examination to overcome the above limitations, including unenhanced magnetic resonance imaging (UMRI). By combining T1-weighted and/or T2-weighted anatomic images with diffusion-weighted imaging (DWI), UMRI candidates as a faster, cheaper, and safer tool to detect and characterize BC [16–23]. DWI exploits the restriction of water molecules diffusivity occurring in BC environment as compared to normal breast tissue. This translates into high tumor-to-normal tissue contrast, with high signal intensity of cancer foci on DWI images, and hypointensity on a set of complementary images calculated after the acquisition, named the Apparent Diffusion Coefficient (ADC) map [24]. In previous works, UMRI provided less sensitivity and specificity than CEMRI, though not at a clinically relevant extent [17,18,20,22,23]. Nevertheless, as far as we know no prior studies investigated whether the combination of UMRI with other imaging modalities can increase diagnostic accuracy and approximate CEMRI in the preoperative setting. We hypothesized that digital breast tomosynthesis (DBT) might complement UMRI effectively. This imaging techniques uses X-ray exposure to produce multiple thin slices of the breast, thus limiting the effects of tissue superimposition which can mask or mimic BC on digital mammography [25]. DBT has shown greater accuracy than digital mammography in assessing BC size and identifying additional disease [26,27]. One might assume that combined UMRI and DBT (UMRI + DBT) can emphasize the advantages inherent to each technique, i.e. high contrast resolution for UMRI, and high spatial resolution for DBT, respectively.

In this light, the main purpose of this study was to compare CEMRI and UMRI + DBT in the preoperative assessment of BC in terms of cancer detection (index lesions and multicentric/multifocal cancer foci) and cancer size estimation.

2. Patients and methods

2.1. Study population and standard of reference

The referring Institutional Review Board approved this study, waiving for the acquisition of the informed consent because of the retrospective design.

By performing a search between January 2016–February 2017, we identified all the women referred to surgery for biopsy-proven BC who underwent preoperative CEMRI, as required by the policy of our tertiary referral institution. Of 514 subjects, we excluded those addressed to neoadjuvant therapy after MRI (n = 7) or showing post-biopsy changes such as clip-related susceptibility artefacts, seroma or haemorrhage (n = 128). Other 323 women were excluded because they did not underwent DBT as prior first-line imaging, or underwent it monolaterally. Final population included 56 women with bilateral CEMRI and DBT, presenting a total of 58 index lesions (i.e., lesions initially prompting CEMRI), and 12 additional lesions confirmed by subsequent ultrasound-guided biopsy and/or final pathological examination after surgery. Of 56 women, 2 showed bilateral index lesions. Among additional lesions, 9 were found in the same breast quadrant of the index lesion, while 3 were in a different quadrant. Women showed a mean age of 58.8 years (±12.3 standard deviation, range 33–81 years).

Pathological analysis was the standard of reference for imaging findings included in the surgical specimen. Analysis was performed by a pool of three pathologists with 5–25 years of experience in breast pathology, who processed surgical specimens and measured cancer according to the College of American Pathologists guidelines valid at the time in which surgery was performed (January 2016–February 2017) [28,29]. Imaging follow-up of at least 2 years served as surrogate standard of reference for those findings not included in the surgical specimen and assessed as benign (see below). Imaging included variable combinations of mammography, ultrasound, DBT and CEMRI.

2.2. Imaging protocols

DBT was acquired on one of two digital mammography systems: Giotto TOMO (Internazionale Medico Scientifica, Bologna, Italy); AW5000 3D Selenia Dimensions (Hologic, Bedford, MA, USA). Each breast was investigated with standard cranio-caudal and medio-lateral oblique views, with both systems generating synthetic two-dimensional (2D) images (s2D) for each view. Table 1 in Appendix A shows the acquisition parameters of DBT.

CEMRI examinations were performed in the prone position on one of two 1.5 T magnets: Magnetom Avanto or Magnetom Aera (Siemens Medical Solutions, Erlangen, Germany), using a bilateral breast 4-channel or 16-channel coil, respectively. The CEMRI protocol, which included DWI, pre- and post-contrast T1-weighted dynamic contrast enhanced imaging (DCE), and T2-weighted imaging, is detailed in Table 2 of Appendix A. Using a remote control injector (OptiStar Elite injector, Mallinckrodt, UK), we administered gadobenate dimeglumine (Multihance, Bracco, Milan, Italy) intravenously, at a dose of 0.1 mmol/kg and an injection rate of 2 ml/s.

2.3. Image analysis

A study coordinator with 4 years of experience in breast imaging, not involved in image analysis, organized reading sessions on our picture archiving and communication system (PACS) workstation (SuitEstensa, Ebit AET, Esaote, Genoa, Italy). ADC maps were generated by the vendor's software (Leonardo Syngo, Siemens Medical Systems, Erlangen, Germany). Cases were prompted during independent and separate reading sessions to three different readers, including a senior radiologist (R1), and two residents (R2 and R3). R1, R2 and R3 showed 10, 3 and 3 years of experience in CEMRI and DBT, respectively. Readers were aware of interpreting preoperative examinations, though they were blinded to prior imaging and clinical information (including lesions' number and type). They accessed two types of examinations: CEMRI alone (including all the sequences reported in Table 2 of Appendix A) or UMRI + DBT. While DBT included native and s2D images for each view, UMRI was composed by the unenhanced T1-weighted sequence and DWI. DWI included the following sets of images: 1) images obtained with low diffusion-weighting (so called low b-

Table 1
Histological type and size of the seventy malignant lesions included in the analysis. IQR = interquartile range; IDC = invasive ductal carcinoma; DCIS = ductal carcinoma in situ; IDLC = mixed invasive ductal-lobular carcinoma; ILC = invasive lobular carcinoma; LCIS = lobular carcinoma in situ. The table note shows the number (n) of histological grades of IDC, IDC with associated in situ component, DCIS, and DCIS associated to invasive cancer.

Type of lesions		Histological type	Number of lesions (% on the total of lesions)	Median size (cm)	IQR
Index cancers (n = 58)		IDC[a]	30 (42.6%)	2.2	13.5–30.0
		IDC[d]+DCIS[b]	18 (25.7%)	1.1	9.0–15.0
		IDLC	4 (5.7%)	2.8	16.0–41.0
		ILC	1 (1.4%)	1.3	–
		ILC + LCIS	1 (1.4%)	2.1	–
		DCIS[a]	4 (5.7%)	6.0	32.0–92.5
Additional cancers (n = 12)	Multifocal cancers	IDC[c]	8 (11.4%)	0.9	8.5–12.0
		IDC[d]+DCIS[b]	1 (1.4%)	0.6	–
	Multicentric cancers	IDC[c]	2 (2.9%)	1.0	–
		DCIS[a]	1 (1.4%)	0.4	–

[a] DCIS: grade 1 (n = 1), grade 2 (n = 2), and grade 3 (n = 2).
[b] DCIS component associated to invasive cancer: grade 1 (n = 3), grade 2 (n = 7), and grade 3 (n = 6).
[c] IDC: grade 1 (n = 4), grade 2 (n = 20), grade 3 (n = 16).
[d] IDC with associated in situ component: grade 1 (n = 4), grade 2 (n = 13), grade 3 (n = 2).

Table 2
Per-reader distribution of the sensitivity, true positive (TP), false negative (FN), and false positive (FP) cases achieved with contrast-enhanced magnetic resonance imaging (CEMRI) versus the combination of unenhanced magnetic resonance imaging (UMRI) and digital breast tomosynthesis (DBT). Denominators of the ratios provided in the rows represent the total number of TP + FN + FP cases.

	Reader 1			Reader 2			Reader 3		
	CEMRI	UMRI + DBT	p[a]	CEMRI	UMRI + DBT	p[a]	CEMRI	UMRI + DBT	p[a]
Sensitivity % (95%C.I.)	100 (0.95–1.00)	88.6 (0.79–0.94)	0.008	94.3 (0.87–0.98)	87.1 (0.77–0.93)	0.180	94.3 (0.87–0.98)	85.7 (0.75–0.92)	0.180
TP	70/92	62/75	0.342	66/95	61/75	0.109	66/88	60/74	0.448
FN	0/92	8/75	0.001	4/95	9/75	0.008	4/88	10/74	0.052
FP	22/92	5/75	0.002	25/95	5/75	0.001	18/88	4/74	0.005

[a] Significance of the intra-reader comparison between CEMRI versus UMRI + DBT.

value images), which are indispensable to build the ADC map; 2) images with strong diffusion-weighting (so called high b-value images), which show the highest tumor-to-normal tissue contrast; 3) the ADC map, obtained from low b value and high b-value images, representing the spatial distribution of the ADC as a measure of water diffusion in the tissue (the term "apparent" accounts for several tissue effects making this index different from pure diffusion coefficient [24]). CEMRI or UMRI + DBT dataset were presented randomly by separating the readings performed on the same women by an interval of time of ≥3 weeks between the two imaging sets.

For each patient, R1-R3 recorded the site (side and quadrant) and size (cm) of imaging findings, categorizing them with the Breast Imaging Reporting and Data System (BI-RADS) for CEMRI and DBT [24]. Findings were assessed as malignant if scored ≥4. BI-RADS categorization included also the assessment of breast density on DBT, and the degree of breast parenchymal enhancement (BPE) on CEMRI [30]. For the purpose of analysis, breast density and BPE were defined as "high" when categorized ≥ C and moderate-to-marked, respectively. Since the BI-RADS is inapplicable to UMRI, readers referred to the categorization score illustrated in Fig. 1. When interpreting UMRI + DBT, a finding was considered as malignant if assessed as category 4 or larger with at least one of the two imaging modalities.

Cancer size was measured on the slice showing the largest diameter when reading CEMRI or DBT. Measurement was performed in the subtracted series showing better lesion conspicuity in the case of CEMRI, and on the view in which the lesion showed better visibility in the case of DBT. Spiculae were excluded from measurement on either CEMRI or DBT [31,32]. On UMRI, lesion measurement was performed on the slice and image (T1-weighted, high b-value or ADC map) where the observation showed maximum conspicuity and diameter.

2.4. Statistical analysis

After assessing data normality with the Shapiro-Wilk test, we reported continuous variables as median and interquartile range (IQR) values. Proportions were reported together with 95% confidence intervals (95%CI).

We calculated the sensitivity for each reader, defined as the percent ratio between true positive (TP) cases and the sum of TP and false negative (FN) cases. On an intra-reader basis, we assessed whether there was any significant difference between CEMRI and UMRI + DBT in terms of sensitivity (using the McNemar test), as well as in the number of TP or FP or FN cases over the total number of TP + FP + FN cases (using the Fisher exact test).

Concerning cancer size, we evaluated CEMRI, DBT and UMRI separately and on an intra-reader basis. Using the Friedman test, we assessed whether there was any significant difference in estimating the size of TP findings that there were detected by all imaging modalities. On the same set of findings, we used Bland-Altman analysis to exploit the agreement of each imaging modality with pathological size. Data underwent logarithmic transformation to match the prerequisites of analysis [33,34], so that mean bias and 95% limits of agreement between measurements were presented as dimensionless values. Bland-Altman analysis was integrated with the intraclass correlation coefficient (ICC), using the following reference values for the agreement [35]: ≤0.40 = poor; 0.40–0.59 = fair; 0.60–0.74 = good; 0.75–1.00 = excellent.

Finally, we built two stepwise logistic regression models for determining which clinical or imaging variable was predictive of

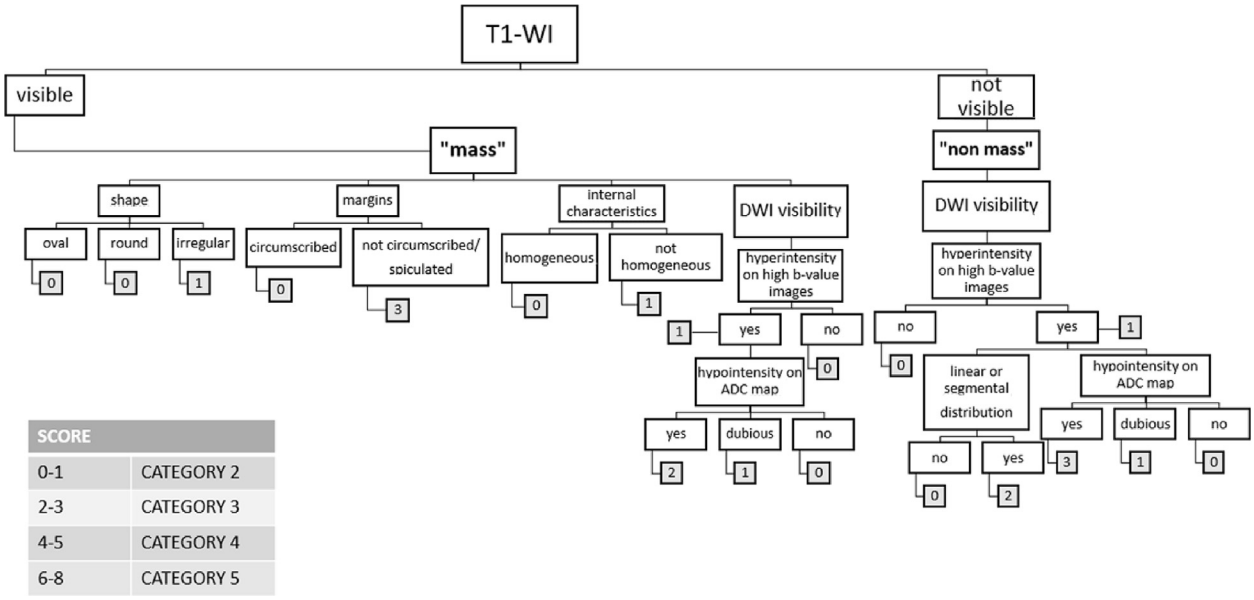

Fig. 1. Flowchart of the interpreting rules for unenhanced magnetic resonance imaging (UMRI). After evaluating whether the UMRI finding showed "mass" or "non mass" appearance on T1-weightening (T1-WI), readers attributed the reported score according to the presentation of each image feature (shape, margins, internal characteristics, appearance on diffusion-weighted imaging [DWI]), until the bottom step was reached. The final score resulted from the sum of each individual score in order to express the risk for malignancy as follows: final score 0–1 = category 2, definitively benign; final score 2–3 = category 3, probably benign; final score 4–5 = category 4, suspicious of malignancy; final score ≥6 = category 5, high suspicious of malignancy. Findings categorized 4 or larger were assumed to be malignant.

missing cancer by at least one of the three readers when using CEMRI or UMRI + DBT.

Analysis was performed on a commercially available software (MedCalc Software bvba, version 18.11.6, Ostend, Belgium). Alfa level was set 0.05, using the Bonferroni correction in the case of multiple pairwise comparisons.

3. Results

3.1. Cancers characteristics

Included women (n = 56) underwent unilateral mastectomy in 33 cases, bilateral mastectomy in 1 case, unilateral breast-conserving surgery in 21 cases, and bilateral breast-conserving surgery in 1 case, respectively.

Table 1 shows the histological type and size of 70 breast cancers found at pathological examination. Median size of all lesions, index lesions alone, and additional lesions alone was 1.5 cm (IQR 0.9–3.0 cm), 1.8 cm (IQR 1.1–3.0 cm) and 0.7 cm (IQR 0.5–1.1 cm), respectively. Overall, cancers size was ≤1.0 cm in 22/70 lesions (31.4%), corresponding to 14/58 index lesions, and 8/12 additional lesions.

3.2. Sensitivity for breast cancer

As shown in Table 2, CEMRI showed higher sensitivity for BC than UMRI + DBT (range 94.3–100% versus 85.7–88.6%). The difference was statistically significant (p = 0.008) in the case of R1 only. FNs induced by UMRI + DBT were significantly (p = 0.001–0.008) or nearly significantly (p = 0.052) larger in number than those induced by CEMRI for R1-R2 and R3, respectively.

Higher sensitivity of CEMRI was counterbalanced by a significantly larger number of FPs compared to UMRI + DBT, regardless of the reader (p ranging 0.001–0.005). There was no significant difference in the number of TPs achieved by both imaging modalities for each reader. The distribution and characteristics of FN and FP findings are detailed in Table 3 Appendix A. FP cases were confirmed by core needle biopsy (CNB), pathological examination if included in the surgical specimen, or imaging follow-up, as detailed in Table 3 in Appendix A. All the FP cases included in the surgical specimen were operated at the time of primary surgery, except for one B3 lesion found by core needle biopsy (identified by R2 only in the study), which underwent lumpectomy separately (no atypia at pathological examination).

Most of CEMRI-induced FPs were avoided by UMRI + DBT, i.e. 21/22 (95.4%) for R1, 24/25 (96.0%) for R2, and 17/18 (94.4%) for R3. Exemplificative cases are shown in Figs. 2–3.

Overall, CEMRI and UMRI + DBT agreed in categorizing cancers with a score ≥4 in 62/70 cases for R1 (88.6%; 95%CI 78.2–94.6), 59/70 cases for R2 (84.3%; 95%CI 73.2–91.5), and 56/70 for R3 (80.0%; 95%CI 68.4–88.3). Agreement in categorizing a finding as suspicious was not investigated with Cohen's kappa statistic because of the low number of ≤3 assignments attributed in common by the two imaging strategies (0 for R1 and R3, and 2 for R2).

The number of benign findings identified by R1, R2 and R3 was 20 in 18 women, 28 in 15 women, and 23 in 14 women using CEMRI, and 19 in 17 women, 20 in 18 women and 22 in 16 women using UMRI + DBT, respectively. None of those findings was shown to be malignant over time.

3.3. Cancer size

Median (IQR) size of category ≥4 findings on CEMRI, DBT and UMRI was 1.5 cm (1.0–3.2), 2.1 cm (1.0–3.0) and 2.0–05 cm (1.3–3.0) for R1; 1.7 cm (1.1–3.0), 2.0 cm (1.1–3.0) and 2.0 cm (1.3–3.0) for R2; 1.7 cm (1.1–3.0), 1.8 cm (1.1–2.8) and 2.0 cm (1.0–3.0) for R3, respectively.

Lesions detected by all imaging modalities were 51/70 for R1, 53/70 for R2, and 43/70 for R3. Among them, there was no significant difference in size between CEMRI, DBT and UMRI (p = 0.328–0.826) as interpreted by R1 (median/IQR 2.3/1.3–3.6 cm, 2.2/1.6–3.0 cm, and 2.1/1.4–3.1 cm, respectively) and R2 (median/IQR 2.2/1.3–3.1 cm, 2.0/1.1–3.0 cm and 2.1/1.3–3.3 cm,

Table 3
Main characteristics of false negative (FN) and false-positive (FP) cancers achieved by contrast-enhanced magnetic resonance imaging (CEMRI) and unenhanced magnetic resonance imaging plus digital breast tomosynthesis (UMRI + DBT). IQR = interquartile range; IDC = invasive ductal carcinoma; DCIS = ductal carcinoma in situ; IDLC = mixed invasive ductal-lobular carcinoma; G1 = grade 1; G2 = grade 2; G3 = grade 3.

		CEMRI		UMRI + DBT		CEMRI and UMRI + DBT	
		FN cancers	FP cancers	FN cancers	FP cancers	FNs in common	FPs in common
Reader 1	Number	0	22	8	5	0	1
	Histological type	–	–	5 IDC G2, 1 IDC G3, 1 ICD G1+DCIS G2, 1 IDC G2+DCIS G2	–	–	–
	Median size (IQR) (cm)	–	1.5 (0.7–2.6)	0.7 (0.5–0.7)	0.8 (0.8–2.3)	–	–
Reader 2	Number	4	25	9	5	2	1
	Histological type	1 IDC G2, 1 IDC G3, 1 IDC G2+DCIS G1, 1 IDLC G2	–	4 IDC G2, 1 IDC G3, 1 DCIS G2, 1 DCIS G3, 1 IDC G2+DCIS G3, 1 IDLC G2	–	1 IDC, 1 IDLC	–
	Median size (IQR) (cm)	0.8 (0.6–0.9)	1.1 (0.9–1.8)	0.7 (0.5–0.8)	1.0 (0.9–1.9)	0.5	–
Reader 3	Number	4	18	10	4	0	1
	Histological type	2 IDC G2, 1 IDC G3, 1 DCIS G3	–	5 IDC G2, 1 IDC G3, 1 DCIS G2, 1 DCIS G3, 1 IDC G1+DCIS G2, 1 IDC G2+DCIS G2	–	–	–
	Median size (IQR) (cm)	2.5 (0.8–5.1)	0.9 (0.7–1.5)	0.7 (0.6–1.4)	1.2 (0.9–1.8)	–	–

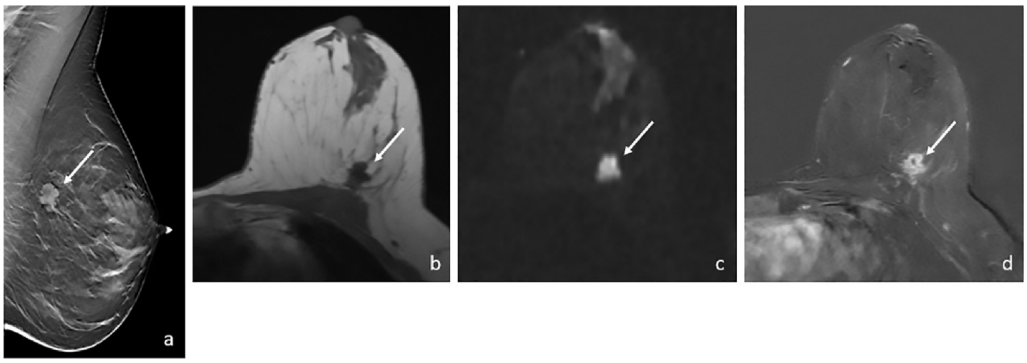

Fig. 2. Concordance in assessing cancer between contrast-enhanced magnetic resonance imaging (CEMRI) CEMRI and unenhanced MRI plus digital breast tomosynthesis (UMRI + DBT) in a 64-years-old patient with unifocal pathology-proven invasive ductal carcinoma. DBT showed a spiculated mass in the left breast, as evident in the medio-lateral oblique view (arrow in a). On UMRI, the mass appeared as a well-conspicuous, spiculated hypointense lesion on T1-weighted transverse imaging (arrow in b), with restricted diffusion on the transverse high b-value image (arrow in c) (apparent diffusion coefficient map not shown). On the CEMRI subtracted T1-weighted imaging (arrow in d), the lesion appeared as a mass with intense contrast enhancement.

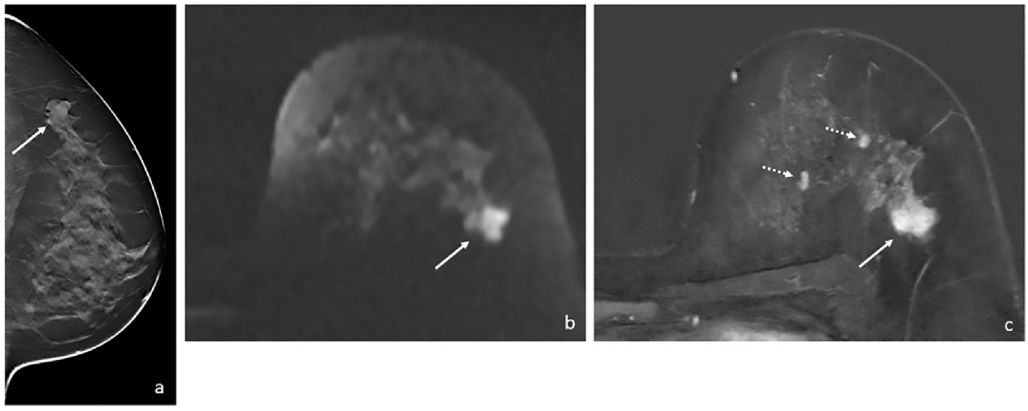

Fig. 3. Discordance between CEMRI and UMRI + DBT in a 51-years-old woman with invasive ductal carcinoma (G3). UMRI + DBT showed a single lesion in the upper-outer quadrant of left breast, presenting as a spiculated mass on DBT (arrow in a) and with hyperintensity on transverse diffusion weighted imaging (b-value 1000 s/mm^2) (arrow in b). On CEMRI, transverse T1-weighted post-contrast subtracted image confirmed the lesion (arrow in c) while showing two additional foci of contrast enhancement on the same breast (<5 mm in diameter), interpreted as suspicious by the readers (dotted arrows in c). Additional findings were finally assessed as false positives, being not confirmed at subsequent second-look ultrasound and final pathology.

respectively). In the case of R3, CEMRI provided significantly ($p = 0.002$) larger size (median/IQR 2.2/1.3–3.1 cm) than DBT (median/IQR 1.9/1.3–2.9 cm) and UMRI (median/IQR 2.0/1.4–3.1 cm).

The results from agreement analysis (Fig. 4) showed that, regardless of the reader, UMRI alone showed narrower limits of agreement and higher ICC values compared, in the descending order, to CEMRI and DBT alone. ICCs showed a similar trend (Fig. 4),

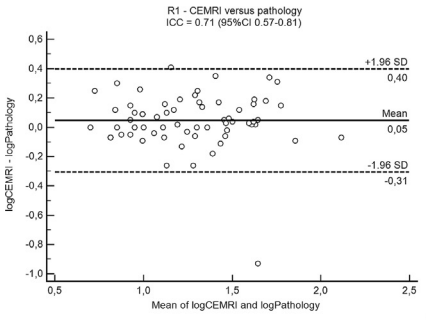
R1 - CEMRI versus pathology
ICC = 0.71 (95%CI 0.57-0.81)
+1.96 SD
0,40
Mean
0,05
-1.96 SD
-0,31
logCEMRI - logPathology
Mean of logCEMRI and logPathology

A

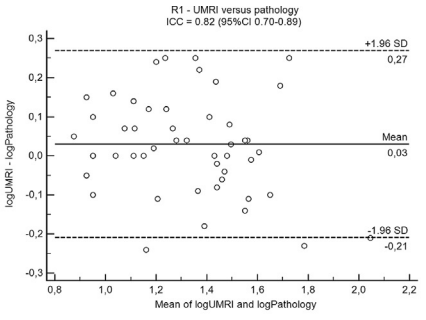
R1 - UMRI versus pathology
ICC = 0.82 (95%CI 0.70-0.89)
+1.96 SD
0,27
Mean
0,03
-1.96 SD
-0,21
logUMRI - logPathology
Mean of logUMRI and logPathology

B

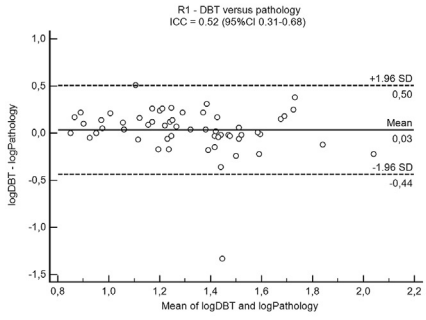
R1 - DBT versus pathology
ICC = 0.52 (95%CI 0.31-0.68)
+1.96 SD
0,50
Mean
0,03
-1.96 SD
-0,44
logDBT - logPathology
Mean of logDBT and logPathology

C

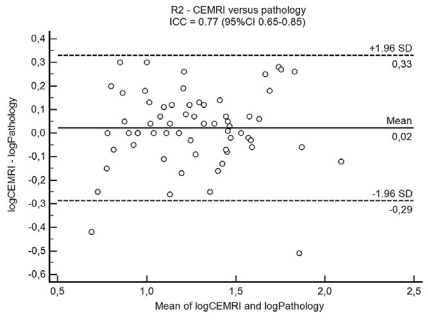
R2 - CEMRI versus pathology
ICC = 0.77 (95%CI 0.65-0.85)
+1.96 SD
0,33
Mean
0,02
-1.96 SD
-0,29
logCEMRI - logPathology
Mean of logCEMRI and logPathology

D

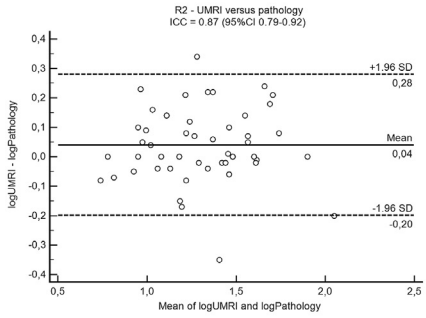
R2 - UMRI versus pathology
ICC = 0.87 (95%CI 0.79-0.92)
+1.96 SD
0,28
Mean
0,04
-1.96 SD
-0,20
logUMRI - logPathology
Mean of logUMRI and logPathology

E

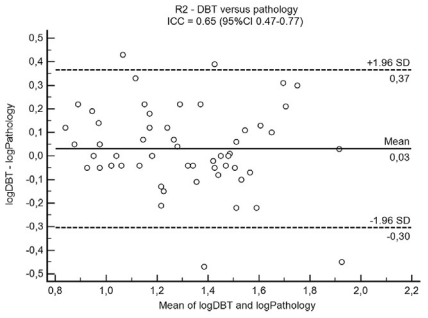
R2 - DBT versus pathology
ICC = 0.65 (95%CI 0.47-0.77)
+1.96 SD
0,37
Mean
0,03
-1.96 SD
-0,30
logDBT - logPathology
Mean of logDBT and logPathology

F

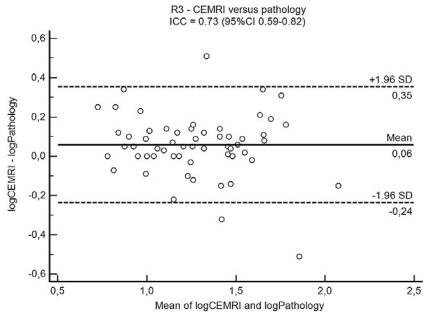
R3 - CEMRI versus pathology
ICC = 0.73 (95%CI 0.59-0.82)
+1.96 SD
0,35
Mean
0,06
-1.96 SD
-0,24
logCEMRI - logPathology
Mean of logCEMRI and logPathology

G

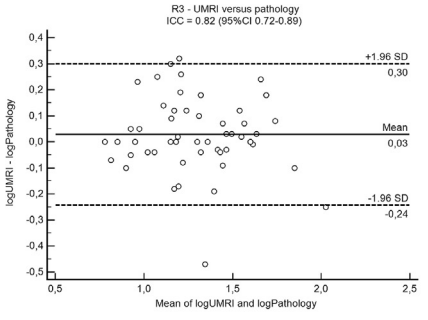
R3 - UMRI versus pathology
ICC = 0.82 (95%CI 0.72-0.89)
+1.96 SD
0,30
Mean
0,03
-1.96 SD
-0,24
logUMRI - logPathology
Mean of logUMRI and logPathology

H

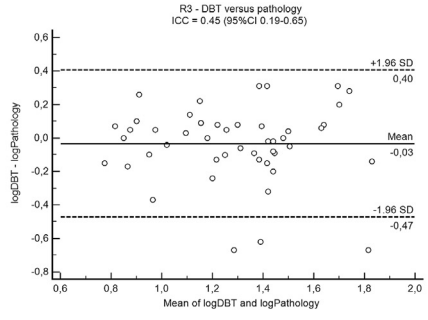
R3 - DBT versus pathology
ICC = 0.45 (95%CI 0.19-0.65)
+1.96 SD
0,40
Mean
-0,03
-1.96 SD
-0,47
logDBT - logPathology
Mean of logDBT and logPathology

I

with R1-R3 values in the range of excellent agreement for UMRI (0.82–0.87) versus good agreement for CEMRI (0.71–0.77), and fair-to-good agreement for DBT (0.45–0.65). Mean bias at Bland-Altman analysis was minimal, regardless of the imaging method.

3.4. Cancer missing

The number and main characteristic of cancers missed by each reader are reported in Table 3. Cancers missed by at least one reader were 8/70 for CEMRI, and 12/70 for UMRI + DBT, respectively.

All readers categorized breast density as BI-RADS B, C and D in 8/56, 34/56, and 14/56 patients, respectively. Readers agreed also in assessing BPE as minimal in 32/56 women, mild in 10/56 women, moderate in 11/56 women, and marked in 3/56 women, respectively.

At multivariate analysis (Table 4), smaller lesions size ($\leq$1.0 cm) was the only independent predictor of missing cancer for both CEMRI and UMRI + DBT, though odds ratio (OR) values showed wide 95%CIs.

4. Discussion

In our study, the sensitivity of UMRI + DBT in the preoperative assessment of BC was high (range 85.7–88.6%), even if inferior to that of CEMRI (range 94.3–100%). The difference was statistically significant in the case of the most experienced readers (R1) only ($p = 0.008$), possibly because less experienced readers missed more cancers even when using the standard imaging of CEMRI, thus reducing the gap in sensitivity as compared to UMRI + DBT. However, CEMRI provided a nearly significant-to-significant ($p = 0.001–0.052$) lower number of FN cases, regardless of the reader. On the bright side, all readers achieved significantly ($p = 0.001–0.005$) less FP findings than CEMRI when using UMRI + DBT. Our results suggest that UMRI + DBT can be a reliable diagnostic alternative to CEMRI in the preoperative assessment of BC, while carrying some specific advantages of UMRI. Indeed, UMRI is a mean to reduce the acquisition time and costs related to contrast medium administration [36]. Its use might potentially increase the accessibility to preoperative breast MRI, and in turn expand current indications [37]. Moreover, avoiding contrast administration would eliminate safety concerns, as exemplified at best in those patients in which gadolinium chelates should be used with caution because of impaired renal function, risk for adverse reaction, or risk for accumulation in the central nervous system [14,15].

Results on sensitivity were expected, given the well-known superiority of CEMRI in detecting foci of tumoral neoangiogenesis [1–3]. Not surprisingly, they are in line with previous studies comparing UMRI alone versus CEMRI, either using different unenhanced protocols (range of sensitivity 50.0–93.8% versus 86.0–98.%, respectively) [17,18,20,22,23], or investigating a similar combination of a T1-weighted sequence and DWI (range of sensitivity 78.4–91.6%) [16,23]. However, we found that the absolute concordance rate between the two imaging strategies was comparably high across the readers (range 80.0–88.6%), suggesting a substantial and reproducible agreement in categorizing imaging findings, regardless of the radiologist's experience.

We did not calculate specificity, given the ambiguity of this index in a context with 100% cancer prevalence. However, our results on FP findings are reasonably in contrast with previous results on specificity. While DBT was shown to be more specific than CEMRI (88.2% versus 74.2%) [38], UMRI alone showed overlapping or even lower specificity in studies of direct comparison with CEMRI (range 71.4–89.3% versus 76.8–92.8%). A possible explanation for the discrepancy is that, differently from those studies, readers were aware of interpreting preoperative examinations, and in turn of the presence of BC. This scenario was affected by the unavoidable detection bias related to the higher likelihood that an imaging finding was malignant [39]. In this scenario, which reflects clinical practice, UMRI + DBT avoided most FPs induced by CEMRI, at a comparable extent in all readers. It should be pointed that the median size of CEMRI-induced FPs was small (range 0.9–1.5 cm for R1-R3). This finding matches with the results of logistic regression, showing that smaller BC size was the only independent predictor of cancer missing, at a larger extent for UMRI + DBT than CEMRI (OR 19.16 versus 8.62, respectively). Our results suggest that UMRI + DBT has the potential of avoiding small FPs induced by CEMRI, and in turn reducing additional "second-look" imaging or biopsy needed for ruling out malignancy [10–12]. This would further limit costs, patient anxiety, and the overall time from diagnosis to surgery, though the role for UMRI + DBT in this setting should be confirmed in further studies.

One might ask which imaging should represent the reference for providing cancer size when using combined UMRI and DBT. According to Bland-Altman analysis, both techniques showed slight mean bias versus pathology, though UMRI provided closer limits of agreement, i.e. minor expected discrepancy compared to pathological size. This result was reasonably related to the higher tumor-to-normal tissue contrast that is achieved with DWI, in which cancer tends to appear as a hyperintense focus over a low-signal background on high b-value images [17]. Regardless of the readers and their experience, UMRI predicted pathological size better than CEMRI, both in terms of limits of agreement and ICCs (range moderate-to-excellent). A possible explanation is that the absence of contrast avoided peritumoral inflammation-related enhancement as a source of size overestimation [40,41]. This hypothesis is in line with larger lesion size we observed with CEMRI than UMRI.

This study suffers from several limitations. First, we excluded a large number of patients (n = 128) with post-biopsy artefacts on CEMRI (and in turn UMRI), thus potentially limiting the applicability of our results to the real clinical scenario, in which the examination is usually performed after breast biopsy. Including those patient was at risk of unblinding the readings by showing the site of the index lesion, which corresponds by definition to that of the artefact. We believe this limitation further emphasizes the potential benefit of preoperative combination of DBT and UMRI, since the former, which is usually available as a pre-biopsy examination, might compensate for the artefacts affecting UMRI. Second, we did not weight the relative impact of UMRI and DBT in providing final diagnosis, thus making difficult to understand the differential role in the combined imaging strategy. However, it is reasonably assuming that main role for UMRI was cancer detection, given high contrast resolution inherent to the technique (especially DWI), while DBT better exploited lesions' morphology. Of note, higher breast density did not impair cancer detection according to multivariate analysis, suggesting that lesions potentially missed by DBT can be complementary diagnosed by UMRI, whose image contrast is inherently unaffected by the amount of fibroglandular tissue. Finally, our study prevalently included invasive ductal carcinomas,

Fig. 4. Bland-Altman plots of cancer size measurements obtained by CEMRI, UMRI and DBT for reader 1 (R1) (a–c), reader 2 (R2) (d–f), and reader 3 (R3) (g–h). Mean bias and limits of agreement compared to pathology are reported as dimensionless values given logarithmic transformation. Intraclass correlation coefficient (ICC) values are reported too, together with 95% confidence intervals (95%C.I.).

Table 4
Results of logistic regression analysis aiming to identify predictors of cancer missing. Breast parenchymal enhancement (BPE) was inapplicable to the UMRI + DBT model. OR = odds ratio.

	Lesions missed by CEMRI		Lesions missed by UMRI + DBT	
	Univariate analysis[a]	Multivariate analysis	Univariate analysis[a]	Multivariate analysis
Age	• <49 years 2/16 (12.5%) • 50–69 years 5/32 (15.6%) • >70 years 1/22 (4.5%) p = 0.386	–	• <49 years 4/16 (25%) • 50–69 years 5/32 (15.6%) • >70 years 3/22 (13.6%) p = 0.625	–
High breast density (≥BI-RADS C)	8/48 (16.7%) p = 0.043	–	9/48 (18.7%) p = 0.600	–
High BPE (moderate-to-marked)	2/19 (10.5%) p = 0.885	–	Not included	Non included
Invasive histology	7/65 (10.7%) p = 0.534	–	10/65 (15.4%) p = 0.162	–
Size ≤1.0 cm	6/22 (27.3%) p = 0.005	p = 0.012 OR 8.62 (95%CI 1.58–47.13)	10/22 (45.5%) p < 0.0001	p = 0.0004 OR 19.16 (95%CI 3.69–99.38)
Being an additional lesion	1/12 (8.3%) p = 0.713	–	5/12 (41.6%) p = 0.013	–

[a] Chi-square test.

alone or in combination with non-invasive components, suggesting that the generalizability of our results should be proven in series encompassing a large number of different histological types, especially invasive lobular carcinoma, as well as difficult-to-diagnose lesions with benign-like appearance (e.g., mucinous tumors).

5. Conclusions

Combined UMRI + DBT showed high sensitivity when performing preoperative assessment of BC. Compared to CEMRI, sensitivity was expectedly lower, though UMRI + DBT avoided the large majority of the FPs induced by the former technique. UMRI showed the highest agreement with pathology in terms of cancer size, even with regard to CEMRI, thus appearing as the reference tool to measure BC in the UMRI + DBT approach. BC size ≤1.0 cm was the only independent predictor of missing cancer for both imaging strategies. Based on our results, one might propose UMRI + DBT as an alternative to CEMRI having the potential of increasing the accessibility to preoperative breast MRI, facilitating patients' workup, and reducing contrast-related risks.

Ethical approval

The study was approved by the Institutional Review board. The acquisition of written informed consent from patients was waived because of the retrospective design.

Funding

This research did not receive any specific grant from funding agencies in the public, commercial, or not-for-profit sectors.

Declaration of competing interest

Francesco Sardanelli declares to have received grants from or being member of the speakers' bureau/advisory board for Bayer-Schering, Bracco, and General Electric. All the other authors have no conflict of interest to declare.

Acknowledgments

None.

Appendix A. Supplementary data

Supplementary data to this article can be found online at https://doi.org/10.1016/j.breast.2019.11.013.

References

[1] Barrett T, Brechbiel M, Bernardo M, Choyke PL. MRI of tumor angiogenesis. J Magn Reson Imaging 2007;26:235–49. https://doi.org/10.1002/jmri.20991.
[2] Houssami N, Ciatto S, Macaskill P, et al. Accuracy and surgical impact of magnetic resonance imaging in breast cancer staging: systematic review and meta-analysis in detection of multifocal and multicentric cancer. J Clin Oncol 2008;26:3248–58. http://jco.ascopubs.org/cgi/doi/10.1200/JCO.2007.15.2108.
[3] Brennan ME, Houssami N, Lord S, et al. Magnetic resonance imaging screening of the contralateral breast in women with newly diagnosed breast cancer: systematic review and meta-analysis of incremental cancer detection and impact on surgical management. J Clin Oncol 2009;27:5640–9. http://jco.ascopubs.org/cgi/doi/10.1200/JCO.2008.21.5756.
[4] Luparia A, Mariscotti G, Durando M, et al. Accuracy of tumour size assessment in the preoperative staging of breast cancer: comparison of digital mammography, tomosynthesis, ultrasound and MRI. Radiol Med 2013;118:1119–36. https://doi.org/10.1007/s11547-013-0941-z.
[5] Girometti R, Zanotel M, Londero V, Linda A, Lorenzon M, Zuiani C. Automated breast volume scanner (ABVS) in assessing breast cancer size: a comparison with conventional ultrasound and magnetic resonance imaging. Eur Radiol 2018;28:1000–8. https://doi.org/10.1007/s00330-017-5074-7.
[6] Katz B, Raker C, Edmonson D, Gass J, Stuckey A, Rizack T. Predicting breast tumor size for pre-operative planning: which imaging modality is best? Breast 2017;23(1):52–8. https://doi.org/10.1111/tbj.12680.
[7] Houssami N, Turner RM, Morrow M. Meta-analysis of pre-operative magnetic resonance imaging (MRI) and surgical treatment for breast cancer. Breast Canc Res Treat 2017;165(2):273–83. https://doi.org/10.1007/s10549-017-4324-3.
[8] Fancellu A, Turner RM, Dixon JM, Pinna A, Cottu P, Houssami N. Meta-analysis of the effect of preoperative breast MRI on the surgical management of ductal carcinoma in situ. Br J Surg 2015;102(8):883–93. http://doi.org/10.1007/s10549-017-4324-3.
[9] Clauser P, Mann R, Athanasiou A, Prosch H, Pinker K, Dietzel M, et al. A survey by the European Society of Breast Imaging on the utilisation of breast MRI in clinical practice. Eur Radiol 2018;28(5):1909–18. https://doi.org/10.1007/s00330-017-5121-4.
[10] Kim TH, Kang DK, Jung YS, Kim KS, Yim H. Contralateral enhancing lesions on magnetic resonance imaging in patients with breast cancer: role of second-look sonography and imaging findings of synchronous contralateral cancer. J Ultrasound Med 2012;31:903–13. https://doi.org/10.7863/jum.2012.31.6.903.
[11] Ryu HH, Kim EY, Park YL, Park CH. The predictive value of second-look ultrasound after preoperative breast magnetic resonance imaging. J Breast Dis 2015;3:65–70. https://doi.org/10.14449/jbd.2015.3.2.65.
[12] Spick C, Baltzer P. Diagnostic utility of second-look US for breast lesions identified at MR imaging: systematic review and meta-analysis. Radiology 2014;273:401–9. https://doi.org/10.1148/radiol.14140474.
[13] Perlet C, Heywang-Kobrunner SH, Heinig A, Sittek H, Casselman J, Anderson I, Taourel P. Magnetic resonance-guided, vacuum-assisted breast biopsy: results from a European multicenter study of 538 lesions. Cancer: Interdiscipl Int J Am Cancer Soc 2016;106:982–90. https://doi.org/10.1002/cncr.21720.
[14] Martin DR. Nephrogenic system fibrosis: a radiologist's practical perspective. Eur J Radiol 2008;66:220–4. https://doi.org/10.1016/j.ejrad.2008.01.029.
[15] Runge VM. Safety of the gadolinium-based contrast agents for magnetic resonance imaging, focusing in part on their accumulation in the brain and

especially the dentate nucleus. Investig Radiol 2016;51:273–9. https://doi.org/10.1097/RLI.0000000000000273.
[16] Trimboli RM, Verardi N, Cartia F, et al. Breast cancer detection using double reading of unenhanced MRI including T1-weighted, T2-weighted STIR, and diffusion-weighted imaging: a proof of concept study. Am J Roentgenol AJR 2014;203:674–81. https://doi.org/10.2214/AJR.13.11816.
[17] Baltzer PA, Bickel H, Spick C, et al. Potential of noncontrast magnetic resonance imaging with diffusion-weighted imaging in characterization of breast lesions: intraindividual comparison with dynamic contrast-enhanced magnetic resonance imaging. Investig Radiol 2018;53:229–35. https://doi.org/10.1097/RLI.0000000000000433.
[18] Bickelhaupt S, Tesdorff J, Laun FB, et al. Independent value of image fusion in unenhanced breast MRI using diffusion-weighted and morphological T2-weighted images for lesion characterization in patients with recently detected BI-RADS 4/5 x-ray mammography findings. Eur Radiol 2017;27:562–9. https://doi.org/10.1007/s00330-016-4400-9.
[19] Belli P, Bufi E, Bonatesta A, et al. Unenhanced breast magnetic resonance imaging: detection of breast cancer. Eur Rev Med Pharmacol Sci 2016;20:4220–9.
[20] Telegrafo M, Rella L, Ianora AAS, Angelelli G, Moschetta M. Unenhanced breast MRI (STIR, T2-weighted TSE, DWIBS): an accurate and alternative strategy for detecting and differentiating breast lesions. Magn Reson Imaging 2015;33:951–5. https://doi.org/10.1016/j.mri.2015.06.002.
[21] McDonald ES, Hammersley JA, Chou SHS, et al. Performance of DWI as a rapid unenhanced technique for detecting mammographically occult breast cancer in elevated-risk women with dense breasts. Am J Roentgenol AJR 2016;207:205–16. https://doi.org/10.2214/AJR.15.15873.
[22] Yabuuchi H, Matsuo Y, Sunami S, et al. Detection of non-palpable breast cancer in asymptomatic women by using unenhanced diffusion-weighted and T2-weighted MR imaging: comparison with mammography and dynamic contrast-enhanced MR imaging. Eur Radiol 2011;21:11–7. https://doi.org/10.1007/s00330-010-1890-8.
[23] Shin HJ, Chae EY, Choi WJ, et al. Diagnostic performance of fused diffusion-weighted imaging using unenhanced or postcontrast T1-weighted MR imaging in patients with breast cancer. Medicine (Baltim) 2016;95:e3502. https://doi.org/10.1097/MD.0000000000003502.
[24] lima M, Honda M, Sigmund EE, Ohno Kishimoto A, Kataoka M, Togashi K. Diffusion MRI of the breast: current status and future directions. J Magn Reson Imaging 2019. https://doi.org/10.1002/jmri.26908. Epub ahead of print.
[25] Houssami N, Skaane P. Overview of the evidence on digital breast tomosynthesis in breast cancer detection. Breast 2013;22(2):101–8. https://doi.org/10.1016/j.breast.2013.01.017.
[26] Seo N, Kim HH, Shin HJ, et al. Digital breast tomosynthesis versus full-field digital mammography: comparison of the accuracy of lesion measurement and characterization using specimens. Acta Radiol 2014;55:661–7. https://doi.org/10.1177/0284185113503636.
[27] Marinovich ML, Macaskill P, Bernardi D, et al. Systematic review of agreement between tomosynthesis and pathologic tumor size for newly diagnosed breast cancer and comparison with other imaging tests. Expert Rev Med Devices 2018;15:489–96. https://doi.org/10.1080/17434440.2018.1491306.
[28] College of American Pathologists. Protocol for the examination of specimens from patients with ductal carcinoma in situ (DCIS) of the breast version 3.2.0.0. https://documents.cap.org/protocols/cp-breast-dcis-13protocol-3200.pdf. [Accessed 19 November 2019].
[29] College of American Pathologists. Protocol for the examination of specimens from patients with invasive carcinoma of the breast version 3.3.0.0. https://documents.cap.org/protocols/cp-breast-invasive-2016-v3300.pdf. [Accessed 19 November 2019].
[30] Sickles EA, D'Orsi CJ, Bassett LW, et al. ACR BI-RADS® Atlas, Breast imaging reporting and data system. Reston, VA: ACR; 2013. p. 39–48.
[31] Peppard HR, Nicholson BE, Rochman CM, Merchant JK, Mayo 3rd RC, Harvey JA. Digital breast tomosynthesis in the diagnostic setting: indications and clinical applications. RadioGraphics 2015;35:975–90. https://doi.org/10.1148/rg.2015140204.
[32] Förnvik D, Zackrisson S, Ljungberg O, et al. Breast tomosynthesis: accuracy of tumor measurement compared with digital mammography and ultrasonography. Acta Radiol 2010;51:240–7. https://doi.org/10.3109/02841850903524447.
[33] Giavarina D. Understanding Bland altman analysis. Biochem Med 2015;25:141–51. https://doi.org/10.11613/BM.2015.015.
[34] Bland JM, Altman DG. A note on the use of the intraclass correlation coefficient in the evaluation of agreement between two methods of measurement. Comput Biol Med 1990;20:337–40. https://doi.org/10.1016/0010-4825(90)90013-F.
[35] Cicchetti DV. Guidelines, criteria, and rules of thumb for evaluating normed and standardized assessment instruments in psychology. Psychol Assess 1994;6:284–90. https://doi.org/10.1037/1040-3590.6.4.284.
[36] Eun Sook K, Morris EA. Abbreviated magnetic resonance imaging for breast cancer screening: concept, early results, and considerations. Korean J Radiol 2019;20:533–41. https://doi.org/10.3348/kjr.2018.0722.
[37] Sardanelli F, Boetes C, Borisch B, Decker T, Federico M, Mansel RE, et al. Magnetic resonance imaging of the breast: recommendations from the EUSOMA working group. Eur J Cancer 2010;46(8):1296–316. https://doi.org/10.1016/j.ejca.2010.02.015.
[38] Mariscotti G, Houssami N, Durando M, et al. Accuracy of mammography, digital breast tomosynthesis, ultrasound and MR imaging in preoperative assessment of breast cancer. Anticancer Res 2014;34:1219–25.
[39] Gutierrez RL, DeMartini WB, Eby P, Kurland BF, Peacock S, Lehman CD. Clinical indication and patient age predict likelihood of malignancy in suspicious breast MRI lesions. Acad Radiol 2009;16:1281–5. https://doi.org/10.1016/j.acra.2009.04.012.
[40] Tse GM, Chaiwun B, Wong KT, et al. Magnetic resonance imaging of breast lesions—a pathologic correlation. Breast Canc Res Treat 2007;103:1–10.
[41] Yeh E, Slanetz P, Kopans DB, et al. Prospective comparison of mammography, sonography, and MRI in patients undergoing neoadjuvant chemotherapy for palpable breast cancer. Am J Roentgenol AJR 2005;184:868–77. https://doi.org/10.2214/ajr.184.3.01840868.